NATIONAL AERONAUTICS AND SPACE ADMINISTRATION

Technical Memorandum 33-603

Design and Flight Performance Evaluation of the Mariners 6, 7, and 9 Short-Circuit Current, Open-Circuit Voltage Transducers

Robert E. Patterson

JET PROPULSION LABORATORY

CALIFORNIA INSTITUTE OF TECHNOLOGY

PASADENA, CALIFORNIA

April 15, 1973

NATIONAL AERONAUTICS AND SPACE ADMINISTRATION

Technical Memorandum 33-603

Design and Flight Performance Evaluation of the Mariners 6, 7, and 9 Short-Circuit Current, Open-Circuit Voltage Transducers

Robert E. Patterson

JET PROPULSION LABORATORY
CALIFORNIA INSTITUTE OF TECHNOLOGY
PASADENA, CALIFORNIA

April 15, 1973

Prepared Under Contract No. NAS 7-100
National Aeronautics and Space Administration

PREFACE

The work described in this report was performed by the Guidance and Control Division of the Jet Propulsion Laboratory.

ACKNOWLEDGMENT

The author wishes to acknowledge the efforts of R. Greenwood who calibrated the transducers and greatly assisted with performance predictions and compilation of in-flight data.

CONTENTS

I. Introduction 1

II. Transducer Description 2

III. Transducer Calibration 3

A. Technique 3

B. Calibration Results 4

IV. Error Discussion 6

A. Actual Transducer Output 6

B. Predicted Transducer Output 8

V. I_{sc}-V_{oc} Transducer In-Flight Performance, Actual vs Predicted Output 11

A. Prediction Techniques 11

B. Actual vs Pre-launch Predictions 12

C. Mariner 6, Based on Post-Launch Predictions 13

D. Mariner 7, Based on Post Launch Predictions 14

E. Mariner 9, Based on Post Launch Predictions 15

F. Comparison of Mariners 6, 7, and 9 I_{sc}-V_{oc} Transducers 17

VI. Conclusion 18

VII. Recommendations 19

Reference 20

TABLES

1. I_{sc}, I_{scr} cell temperature coefficients at 50 mW/cm^2 (average from 60° C to 0° C) 21

2. Effect of variations in temperature coefficients on predicted transducer output (intensity = 50 mW/cm^2) . . . 22

3. Deviation of prelaunch predicted from actual on "day 0" . . . 23

CONTENTS (contd)

FIGURES

1. Typical MM'69, MM'71 I_{sc}-V_{oc} transducer 24
2. MM'69, MM'71 solar panel design 24
3. Typical MM'69, MM'71 I_{sc}-V_{oc} transducer test plate. . . . 25
4. Mariner 9 I_{sc}, I_{scr} pre-launch calibration. 25
5. Mariner 9 V_{oc} cell calibration 26
6. Mariner 9 I_{sc} cell calibration extrapolation 26
7. Mariner 9 I_{scr} cell calibration extrapolation. 27
8. Mariner 9 I_{sc} cell temperature correction term 27
9. Mariner 9 I_{scr} cell temperature correction term 28
10. Elements of I_{sc}-V_{oc} transducer and temperature transducer actual output 29
11. Elements of I_{sc}-V_{oc} transducer predictions 30
12. Accuracy in percent for a ±3 percent of full scale channel. 31
13. Mariner 6 intensity-temperature relationship 31
14. Mariner 6 actual and predicted I_{sc} cell output versus time 32
15. Mariner 6 actual and predicted I_{scr} cell output versus time 32
16. Mariner 6 I_{sc}-V_{oc} transducer current degradation 33
17. Mariner 6 actual and predicted V_{oc} cell output versus time 33
18. Mariner 6 V_{oc} cell and C439 temperature versus time . . . 33
19. Mariner 7 intensity-temperature relationship 34
20. Mariner 7 actual and predicted I_{sc} cell output versus time 34
21. Mariner 7 actual and predicted I_{scr} cell output versus time 34

FIGURES (contd)

22. Mariner 7 I_{sc}-V_{oc} transducer current degradation 35

23. Mariner 7 actual and predicted V_{oc} output versus time 35

24. Mariner 7 V_{oc} cell and C439 temperature versus time 35

25. Mariner 9 intensity-temperature relationship 36

26. Mariner 9 actual and predicted I_{sc} cell output versus time . 36

27. Mariner 9 actual and predicted I_{scr} cell output versus time 36

28. Mariner 9 I_{sc}-V_{oc} transducer current degradation 37

29. Mariner 9 actual and predicted V_{oc} cell output versus time 37

30. Mariner 9 V_{oc} cell and C419 temperature versus time 37

31. Mars heating effect with days in orbit as a parameter 38

32. Mars heating effect on channel 423, 419, and 116 during first day of orbit 38

33. Mars heating effect on channel 423, 419 and 116 during 43rd day of orbit 39

34. Mariners 6, 7 and 9 I_{sc}-V_{oc} transducer degradation versus time 39

Appendix 40

Table 1A. Mariner 6 I_{sc}-V_{oc} transducer data (S/N 001, calibrated in air) 41

Table 2A. Mariner 7 I_{sc}-V_{oc} transducer data (S/N 004, calibrated in air) 42

Table 3A. Mariner 9 I_{sc}-V_{oc} transducer data (S/N 021, calibrated in vacuum) 43

ABSTRACT

The purpose of the short-circuit current open-circuit voltage (I_{sc}-V_{oc}) transducer is to provide engineering data to aid the evaluation of array performance during flight. This report describes the design, fabrication and calibration and discusses the in-flight performance of the I_{sc}-V_{oc} transducers on board the Mariner 6, 7 and 9 spacecraft. No significant differences were observed in the in-flight electrical performance of the three transducers (Mariner 6, 7 and 9). There was no evidence of solar flares causing abrupt degradation. No significant particulate radiation cell degradation was observed. The transducers did experience significant "non-cell degradation" which refers to losses due to coverslides or adhesive darkening, increased surface reflection, or spectral shifts within coverslide assembly. Mariner 6, 7 and 9 transducers showed non-cell current degradations of 3-1/2%, 3% and 4%, respectively at Mars encounter and 6%, 3%, and 4-1/2%, respectively at end of mission (Day 720, 640 and 480, respectively). Mariner 9 Solar Array Test 2 (March 29, 1972) offered a unique opportunity to correlate transducer and array performance with respect to electrical performance degradation. The array test showed 3-1/2% current degradation while the transducer showed 4-1/2%. The correlation was good; however, results of the error analysis presented in this paper support the need for more accurate telemetry and transducer calibration data as well as the need to investigate improved devices to directly observe in-flight array characteristics for future spacecraft.

I. INTRODUCTION

The purpose of the short-circuit current open-circuit voltage (I_{sc}-V_{oc}) transducer is to provide engineering data to aid the evaluation of array performance during flight. The in-flight performance of the JPL Mariner spacecraft's solar power sources frequently cannot be directly observed through engineering solar array telemetry data. This is because of the operational characteristics of the power subsystem design and the limitations associated with telemetry channel availability. During those periods when array characteristics are obscured, evaluation of array properties is supported with the use of the I_{sc}-V_{oc} transducer.

Three special standardized solar cells, representative of the solar cells used to fabricate the solar array, serve as the basic transducer components. These cells are loaded with precision resistors having values selected to measure short-circuit current on two of the cells and open-circuit voltage on the remaining cell while at the same time accommodating the telemetry operating range. One of the two short-circuit current cells used in the transducer was bombarded with electrons before assembly to degrade its output approximately 50 percent, which rendered the cell relatively insensitive to further radiation degradation (I_{scr} cell). The intent was to provide an indication of the relative space radiation damage to the transducer; performance of the bombarded cell is compared with that of the short-circuit current cell (I_{sc} cell) not subjected to pre-flight radiation damage.

The concept of an I_{sc}-V_{oc} transducer dates back to the original Ranger (1961) and Mariner (1962) spacecraft. While I_{sc}-V_{oc} transducers were designed and fabricated for these early space vehicles, it was not until the Mariner Mars 1964 (Mariner 4) that meaningful flight information was returned. Since that time, I_{sc}-V_{oc} transducers have been incorporated on

the Mariner 5 and Surveyor 5, 6, and 7 solar panels. More recently, transducers on the Mariner 6 and 7 spacecraft (launched in 1969) have flown by the planet Mars and the transducer on Mariner 9 (launched in 1971) is currently orbiting the planet Mars. The specific purpose of this report is to describe the design, fabrication and calibration, and discuss the in-flight performance of the I_{sc}-V_{oc} transducers on board the Mariner 6, 7 and 9 spacecraft.

II. TRANSDUCER DESCRIPTION

Mariner 6, 7 (MM'69) and 9 (MM'71) I_{sc}-V_{oc} transducers are identical in design. A typical transducer is shown in Fig. 1. Each transducer contains three, 1 cm x 2 cm x 0.046 cm, N/P silicon solar cells. The cells have a base resistivity of 1-3 ohm-cm and employ solder-dipped, silver-titanium contacts. Mariner 6, 7 and 9 transducer solar cells were manufactured by Heliotek and are identical, except for area, to the Mariner 6, 7 and 9 solar panel cells, respectively. Solar panels were fabricated using 2 cm x 2 cm x 0.046 cm cells.

The I_{sc} cell of the transducer is loaded with a 1.5 ohm resistor to permit operation of the cell near its short-circuit current region. The I_{scr} cell is also loaded with a 1.5 ohm resistor, however, this cell was electrically degraded by an electron bombardment of 1×10^{16} e/cm^2 at 1 MeV prior to mounting. The short-circuit current of the I_{scr} cell has therefore been reduced by approximately 50 percent and is relatively insensitive to additional radiation damage as compared to a normal solar cell. The V_{oc} cell is loaded with a 1000 ohm resistor divider network of 900 ohms and 100 ohms in series. Output is taken from across the 100 ohm resistor, thus one-tenth of the true open-circuit voltage is fed to the telemetry channel. The resistive loads are incorporated on the same fiberglass printed circuit board as the transducer cells and are potted in RTV-40 for protection against ultraviolet radiation.

Each of the three cells is covered with a 0.051 cm quartz coverglass having a 4100 Å cuton filter deposited on the side adjacent to the cell and an antireflective coating deposited on the opposite surface. The filters are

manufactured by Optical Coating Laboratory, Inc., and again except for area, are identical to the filters used in the MM'69 and MM'71 solar panel construction.

Production techniques and materials employed to fabricate the I_{sc}-V_{oc} transducers are similar to those used in the solar panel fabrication. The completed transducer is 12.2 cm in length, 1.9 cm in width and measures 0.6 cm at its thickest point. Weight of each transducer is approximately 12 grams.

Output of the I_{sc} and I_{scr} cells is taken to be the voltage drop across the 1.5 Ω resistors and therefore has the units of potential difference (mV). Output of the V_{oc} cell is taken to be 10 times the output across the 100 Ω resistor. These conventions were used during calibration, output predictions, and conversion of digital data from the spacecraft to engineering units. V_{oc}, I_{sc}, and I_{scr} cell data is telemetered on Channels 423, 424, and 425, respectively, which are all 100 mV full scale channels.

Locations of the I_{sc}-V_{oc} transducers on the MM'69 and MM'71 solar panels are identical as shown in Fig. 2. Note that the I_{sc}-V_{oc} transducers are located on the front side of the solar panel and temperature transducers were mounted on the back side. I_{sc}-V_{oc} transducer temperature was determined by the closest temperature transducer (Channel 439 for MM'69 and 419 for MM'71).

III. TRANSDUCER CALIBRATION

A. Technique

Twelve MM'69 I_{sc}-V_{oc} transducers and eight MM'71 I_{sc}-V_{oc} transducers were calibrated. The MM'69 transducers were calibrated in air using a Spectrolab X-25L Solar Simulator. Balloon flight standard cell BFS-409, a 2 cm x 2 cm MM'69 solar cell was used to establish the X-25L simulator intensity throughout the calibration. All BFS cells were standardized on a JPL standardization balloon flight; the cells were flown at 120,000 ft and AM0 data on the cells was telemetered back to earth. The MM'71 transducers were calibrated in vacuum using an X-25 Mark II Solar Simulator and balloon flight standard BFS-510 as an intensity reference.

Four transducers at a time were mechanically bonded to a single temperature controlled test plate. One of the four was a "dummy" transducer which was thermocouple instrumented to aid thermal control during test. Test temperature was considered to be the average of the temperatures indicated by the three thermocouples bonded to the "dummy" transducer. Since the transducers were flight hardware, it was not possible to bond thermocouples to them. A typical test plate is shown in Fig. 3. The MM'69 transducers were calibrated in air at intensities of 139.6, 100, and 50 mW/cm^2 and at temperatures of 8, 28, and 60° C for each intensity. The MM'71 transducers were calibrated in a vacuum test chamber at intensities of 139.6, 100, 70, 60 and 50 mW/cm^2 and at temperatures of 60, 28, and 0 °C at each intensity.

B. Calibration Results

Raw calibration data for Mariner 6, 7 and 9 I_{sc}-V_{oc} transducers are presented in Appendix A (Tables 1, 2 and 3). Utilizing the raw calibration data to arrive at an actual prediction is a somewhat controversial subject as the possible methods are numerous. For example, one can use average calibration of all the transducers or individual calibration data of each transducer. Also, one can subject the raw data to many different degrees of "smoothing." Two methods are described in this report; one was used for pre-launch predictions and one was used for post launch predictions. The Mariner 9 transducer will be used as an example as both Mariner 6 and 7 transducers were handled similarly.

1. Pre-Launch Predictions. For pre-launch predictions, the I_{sc} and I_{scr} calibration data was plotted as a linear function of intensity with temperature as a parameter as shown in Fig. 4. The V_{oc} calibration data was plotted as a function (non-linear) of intensity also with temperature as a parameter as shown in Fig. 5. Below 0 °C the parametric curves were generated by extrapolation. Interpolation was used to generate curves in between calibration data. V_{oc} was assumed to be a linear function of temperature at constant intensity. Pre-launch predictions are made using Figs. 4 and 5 and the predicted trajectory and temperature data.

2. Post-Launch Predictions. For the V_{oc} cell, post launch predictions were made using Fig. 5, the actual trajectory, and in-flight solar

array temperature data from Channel 419 (Channel 439 for MM'69 transducers). Post launch predictions for the I_{sc} and I_{scr} cells were made using the actual trajectory, in flight temperature data from Channel 419, early in flight I_{sc} and I_{scr} data as a reference "Day 0" calibration point, and the calibration scheme described in the paragraphs following.

For post-launch predictions of the I_{sc} and I_{scr} cells, the following analytical expression was used to predict I_{sc} at intensity H and temperature T:

$$I_{sc} = I_{sc_0}\left(\frac{H}{H_0}\right) + \int_{T_0}^{T} \alpha\,(H, T)\,dT \qquad (1)$$

where

Isc = Predicted I_{sc} at temperature T and intensity H

I_{sc_0} = Actual in-flight I_{sc} during first day following launch

H = Intensity corresponding to predicted I_{sc}

H_0 = Actual intensity during first day following launch

T_0 = Actual temperature during first day following launch

T = Temperature corresponding to predicted I_{sc}

$\alpha\,(H, T)$ = Temperature coefficient at intensity H in mV/° C

Note that α is a function of both intensity and temperature as indicated in equation one and thus one cannot linearly extrapolate the calibration data presented in Appendix A to points below 0° C. For the I_{sc} cell, extrapolation was done graphically as shown in Fig. 6 using parametric data of 15 cells similar to the I_{sc} cell as a pattern of behavior below 0° C. Since temperature coefficients of I_{scr} and I_{sc} cells are significantly different, I_{sc} parametric data was not suitable as a pattern for extrapolation of the I_{scr} data. For this reason I_{scr} cell number 015 was calibrated in vacuum

down to temperatures below -30° C. Extrapolation of the I_{scr} cell output is shown in Fig. 7. Figures 6 and 7 show the magnitude of error that would be incurred if I_{sc} and I_{scr} were linearly extrapolated below 0° C. Figures 6 and 7 were replotted as Figs. 8 and 9 with respect to a new reference temperature of 50° C (day 0 temperature for Mariner 9 solar panels). For each parametric intensity plotted in Figs. 8 and 9 a point was plotted corresponding to the actual S/P temperature (C419) experienced at that intensity. A curve was then drawn through these points yielding:

$$\int_{T = 50^\circ C}^{T} \alpha\,(H, T)\, dT$$

where the specific temperature-intensity relationship for the Mariner 9 solar panel has been built into the curve. Thus, for post-launch predictions of the I_{sc} and I_{scr} cells, equation 1 is used together with Figs. 8 and 9.

IV. ERROR DISCUSSION

The apparent performance of the Mariner 6, 7 and 9 I_{sc}-V_{oc} transducers is determined by comparing their actual and predicted outputs. In order to determine the significance of variations in actual and predicted performance it is necessary to consider composite errors associated with the actual I_{sc}-V_{oc} transducer and temperature transducer output and the predicted I_{sc}-V_{oc} transducer output. Elements of the actual and predicted transducer outputs are summarized in Figs. 10 and 11, respectively. Errors associated with these elements are discussed in the paragraphs following.

A. Actual Transducer Output

Major elements of the actual transducer output include analog to digital conversion and smoothing of the raw data following conversion to engineering units from telemetered data numbers.

1. A to D Conversion. In the JPL "Functional Requirement Mariner Mars 1971" (M71-4-2006A) it states that the accuracy of a measurement as

read from the input of the FTS to the A to D converter output shall be maintained at ±3 percent of full scale for 0 to 100 mV channels. It further states that the accuracy shall be maintained for the mission lifetime requirements and under all specified environmental conditions. Recall that the I_{sc}-V_{oc} transducer channels are 100 mV full scale channels (423, 424, and 425). The impact of ±3 percent of full scale accuracy on the percent of reading over the upper 85 percent of the channel scale is shown in Fig. 12. Note that the accuracy of a reading at mid-band drops to ±6 percent of reading and at 20 percent of full scale drops to ±15 percent of reading. A ±3 percent of full scale accuracy translates to absolute accuracies of ±6.4° C, ±30 mV, ±3 mV and ±3 mV for the temperature transducer (Channel 419), V_{oc} transducer (Channel 423), I_{sc} transducer. (Channel 424) and I_{scr} transducer (Channel 425) respectively, as shown in the insert in Fig. 12. Also shown in the insert are outputs of the 4 transducers at points in the MM'71 mission where outputs took on their largest and smallest values. Although only MM'71 data is shown, the results are practically the same for both MM'69 spacecraft. Worst case percent accuracies of the V_{oc}, I_{sc}, and I_{scr} transducers range from ±4.5 to ±5.7, ±3.1 to ±9.0, and ±5.3 to ±19.2, respectively. Accuracy of the I_{scr} transducer is the lowest because its output is the lowest in magnitude.

At this point it is strongly emphasized that accuracies discussed in the preceding paragraph represent worst case conditions. There is much evidence which indicates that the actual accuracies of Channels 419, 423, 424, and 425 are much better than the "guaranteed" accuracies. Evidence in support of better than "guaranteed" accuracy is that outputs from these Channels (419, 423, 424, 425) and other 100 mV channels are, in general predicted well within the accuracies shown in Fig. 12. Also, data number changes for these channels are seen to occur continuously in accordance with changes in heliocentric distance and temperature and very seldom change more than 1 DN over a normal 24 hour tracking period. One DN on a 100 mV scale is 0.8 mV or 0.8 percent of full scale. One DN on Channel 419 corresponds to 1.5° C.

2. Data Smoothing. The second major element of the actual transducer output is data smoothing following the conversion of data numbers to engineering units. One data word is comprised of 7 binary bits and hence

the transducer data has a 1/128 of full scale resolution corresponding to 0.8 mV or 0.8 percent of full scale. By plotting the transducer data and drawing a smooth curve through the points, the 1/128 resolution can be improved upon somewhat. However, improvement can only be attained when daily tracking is available and when the output has the same DN value for a number of consecutive days. Thus during the mission where daily data is not available and also when no more than two consecutive data points have the same DN value, actual data has a resolution of ±1/2 DN.

3. Summary. Guaranteed accuracy of the I_{sc}-V_{oc} transducer data is ±3 percent of full scale. Much evidence indicates that the guaranteed accuracy is very conservative. Actual accuracy has an upper limit in accordance with data resolution (0.8 percent of full scale). In this report, actual transducer output will never be assumed to be more accurate than ±1/2 DN (0.8 percent of full scale) however, statements will be made based on the assumption that actual transducer output is more accurate than guaranteed accuracy.

B. Predicted Transducer Output

Major elements of the predicted transducer output include the physical parameters incident solar intensity and transducer temperature (inputs to the transducer model), and the I_{sc}-V_{oc} transducer calibration.

1. Solar Intensity. Incident solar intensity is not measured directly, rather it is deduced from the spacecraft heliocentric radius and attitude, and from the intensity model:

$$H = \frac{K}{R^2} \text{Cos } \theta$$

where

H = solar intensity (mW/cm^2)

R = Heliocentric radius (A.U.)

K = Constant (139.6 (mW/cm^2) x (A.U.)^2)

θ = Off normal angle of incident solar radiation

Assuming the trajectory to be accurate to within one part per million and the spacecraft attitude to be accurate to within 0.018 radians, the calculated intensity is accurate to within 0.02 percent. The constant K has been examined by many investigators and there is some slight variation in reported values however, the "exact" value of K is not a critical factor since short circuit current is predicted according to:

$$I_{sc} = I_{sc_0}\left(\frac{H}{H_0}\right) + \int \alpha dT = I_{sc_0}\frac{\left(\frac{K}{R^2}\right)}{\left(\frac{K}{R_0^2}\right)} + \int \alpha dT = I_{sc_0}\left(\frac{R_0^2}{R^2}\right) + \int \alpha dT$$

where K is seen to cancel out of the expression.

2. Temperature. All transducer predictions presented in this report assume that the I_{sc}-V_{oc} transducer is at exactly the same temperature as that indicated by the solar panel temperature transducer. Thus, there are two elements of temperature uncertainty. Since the temperature transducer is located on the back side of the panels and the I_{sc}-V_{oc} transducer is located on the front side of the panels, it is reasonable to assume that the two transducers are not at exactly the same temperature. Also, temperature indicated by the transducer could be different from the actual transducer temperature (worst case ±7° C, best case ±1.5° C). A ±2.5° C temperature uncertainty is assumed which corresponds to approximate uncertainties of ±5.5 mV, ±0.05 mV, and ±0.12 mV in V_{oc}, I_{sc}, and I_{scr}, respectively.

3. Transducer Calibration. During calibration, temperature readout was to within ±1° C, millivolt readout was to within ±0.1 millivolt, and intensity was controlled to within ±1 percent; however, the resultant calibration accuracy is not as high as these component accuracies imply. Table 1 gives some insight into the transducer calibration accuracy where average temperature coefficients, $\bar{\alpha}$, have been computed at 50 mW/cm^2 between 60° and 0° C for various transducers and various groups of transducers. Key points to note are the variations in $\bar{\alpha}_{I_{sc}}$ and $\bar{\alpha}_{I_{scr}}$ between (1) the Mariner '69 and '71 transducers (2) average of all MM'69 transducers and MM'69 flight transducers (SN 001, 004), and (3) average of all MM'71 transducers and MM'71 flight transducer.

Also note that vacuum calibration consistently yields larger temperature coefficients. At this time it is impossible to separate experimental uncertainty and actual physical variations in α. The lower portion of Table 1 shows 3 separate determinations of α for two transducers. The effect of such variations in $\bar{\alpha}$ on the predicted I_{sc} and I_{scr} output is shown in Table 2. A similar analysis of V_{oc} temperature coefficient variation indicated a variation of 2 percent in V_{oc} predicted output. A further consideration is that temperature correction terms had to be extrapolated below 0° down to -30° C. This had very little effect on V_{oc} accuracy since V_{oc} is linear with temperature over the range of mission temperatures. However, as seen in the calibration section of this report, I_{sc} and I_{scr} are not linear functions of temperature at constant intensity below 0° C and consequently one can expect calibration accuracy to degrade as the non-linear functions are extrapolated below 0° C. Compounding the problem of decreasing accuracy below 0° C is the fact that as temperature and intensity decrease, so does I_{sc} and I_{scr} with the temperature correction term getting larger both absolutely and in terms of a percentage of the predicted output. Based on considerations discussed in paragraph IV-A-3 and this section, results presented in Tables 1 and 2, and analysis of the total calibration data obtained, prelaunch and post launch prediction accuracies were determined to be:

Pre-Launch Prediction Accuracies

Assumptions

(1) Transducer temp = 419 predicted temp.

(2) Intensity = K/R^2 where R is the predicted trajectory.

Transducer	Day 0	71 mW/cm^2, 0° C	50 mW/cm^2, -30° C
V_{oc}	±3.5%	±3.5%	±3.5%
I_{sc}	±2%	±4.5%	±5.5%
I_{scr}	±2%	±6%	±8.0%

Post Launch Prediction Accuracies

Assumptions

(1) Transducer temp = channel 419 actual temp.

(2) Intensity = K/R^2 when R is from the actual trajectory.

(3) Equation (1), page 5.

Transducer	Day 0	71 mW/cm^2, 0°C	50 mW/cm^2, -30°C
V_{oc}	±3%	±3%	±3%
I_{sc}	0%	±2.5%	±3.5%
I_{scr}	0%	±4%	±6.0%

V. I_{sc}-V_{oc} TRANSDUCER IN-FLIGHT PERFORMANCE, ACTUAL vs PREDICTED OUTPUT

A. Prediction Techniques

Prediction techniques were thoroughly discussed in Section III and are summarized below.

Pre-launch Predictions: Based on prelaunch trajectory, prelaunch predicted temperatures and prelaunch calibration data.

Post-launch Predictions: Based on actual trajectory, actual temperature (Channel 439 for Mariners 6 and 7, Channel 419 for Mariner 419) and pre-launch calibration data. I_{sc} and I_{scr} predictions are normalized to Day 0 performance in accordance with:

$$I_{sc} = I_{sc_0}\left(\frac{H}{H_0}\right) + \int_{T_o}^{T} \alpha dT$$

where

I_{sc_0} = Actual transducer output on Day 0

H_0 = Intensity on Day 0

T_o = Actual temperature (419 or 439) on Day 0

B. Actual vs Pre-launch Predictions

Pre-launch predicted performance curves were generated in March 69 for Mariner 6 and 7 I_{sc}-V_{oc} transducers and in April of 1971 for Mariner 9 transducer. These curves are not presented in this report, however, Day 0 (first day of mission) performance is summarized in Table 3.

Table 3 shows that in 3 cases out of 9, the predictions were not within the anticipated pre-launch predicted accuracy discussed in Section 4. Since predicted temperatures were very close to actual temperatures on all these spacecraft, the situation is not remedied by correcting the I_{sc}-V_{oc} transducer predictions in accordance with actual temperatures. Deviation trends appear to be very consistent. In all cases the predicted V_{oc} outputs were lower than the actual outputs while the predicted I_{sc} and I_{scr} cell outputs were higher than the actual I_{sc} and I_{scr} cell outputs. For the three transducers, basing the predictions on temperatures up to 4° C lower than that indicated by the temperature transducer would lower the percent deviation on all nine cells. It certainly appears that at earth space conditions the I_{sc}-V_{oc} transducers are slightly lower in temperature than those indicated by the backside temperature transducers. Another consistent data trend noted in Table 3 is that percent deviations for the I_{scr} cells are higher than for the I_{sc} cells. One possible explanation for this trend is that the solar simulator used for calibration cannot exactly duplicate the spectral distribution of space sunlight and irradiated solar cells have their spectral response significantly shifted toward the "red" portion of the solar spectrum. Thus a solar simulator with a slightly higher red blue ratio than AM0 natural sunlight would help explain at least part of the deviation trend noted in Table 3.

C. Mariner 6, Based on Post-Launch Predictions

Mariner 6 post-launch predictions are based on the temperature-intensity vs time relationship displayed in Fig. 13.

1. I_{sc} and I_{scr} Cells, Degradation. Figures 14 and 15 present actual and predicted outputs for the I_{sc} and I_{scr} cells, respectively. Note that following day 0 normalization, actual outputs for both cells are consistently lower than predicted. The ratio of predicted to actual output for both cells was computed periodically through the mission and plotted as a function of time in Fig. 16. A smooth curve is drawn through the points. Since calibration data is extrapolated below 8° C, the smooth curve was drawn to comply closer to data corresponding to S/P temperatures greater than 8° C. If a cell experienced no degradation, and assuming accurate predictions, the smooth curve would be a straight line, all points on the line having the value of unity (actual = predicted at all points). However, Fig. 16 indicates that both the I_{sc} and I_{scr} cells experienced degradation since the smooth curve through the ratios takes on values less than unity. Several important points are noted:

(1) All computed ratios plotted in Fig. 16 do not deviate from the smooth curve by more than the anticipated prediction accuracies discussed in Section IV.

(2) There appears to be no significant difference in degradation experienced by the I_{sc} and I_{scr} cells and hence the cells experienced other than particulate radiation damage. This point will be discussed further in Section V-E.

(3) Behavior of the deviation of data points from the smooth curve in the below 8° C temperature range indicates that the extrapolated temperature correction

$$\int_{T_0}^{T} \alpha \, dT$$

was larger than it should have been.

(4) Degradation appears to be approximately 3-1/2 percent at encounter (Day 157) and 6 percent at the end of mission (Day 720).

2. V_{oc} Cell, Temperature Deviation. Figure 17 presents the actual and predicted output of the V_{oc} cell. Note the 3 crossover points. V_{oc} starts out higher than predicted, crosses over around Day 140. Maximum deviation occurs around day 340 where V_{oc} is more than 10 mV lower than predicted. Deviation of actual V_{oc} from predicted can also be interpreted as a temperature deviation between the V_{oc} transducer and the back side temperature transducer as shown in Fig. 18 where V_{oc} output is converted to indicated temperature and compared to Channel 439 actual temperature. At Day 0 note that the V_{oc} appears to be 3° C cooler than 439, crosses over at 10° C and reaches a maximum deviation of 6° C around Day 340 (coldest point in the mission). As the panels warm up the temperatures converge and good correlation between V_{oc} and Channel 439 temperature is observed above 8° C. However, it is pointed out that deviation between actual and predicted V_{oc} is at all points of the mission within the anticipated accuracy of the V_{oc} output prediction.

D. Mariner 7, Based on Post Launch Predictions

Mariner 7 post-launch predictions are based on the temperature-intensity vs time relationship displayed in Fig. 19.

1. I_{sc}-I_{scr} Cells, Degradation. Figures 20 and 21 present actual and predicted outputs for the I_{sc} and I_{scr} cells, respectively. Note that following Day 0 normalization, actual output is consistently lower than predicted for the I_{sc} cell. The same was true for the I_{scr} cell except between Days 140 to 380 where the predicted output has the greatest uncertainty due to extrapolated calibration. The ratio of predicted to actual output for both cells was computed periodically through the mission and plotted as a function of time in Fig. 22. A smooth curve was drawn through the points such that it complies closer to points corresponding to S/P temperatures greater than 8° C since calibration data is extrapolated below 8° C. Figure 22 indicated that both the I_{sc} and I_{scr} cells experienced degradation. Several important points are noted:

(1) All computed ratios plotted in Fig. 22 do not deviate from the smooth curve by more than the prediction accuracies discussed in Section IV.

(2) There appears to be no significant difference in degradation experienced by the I_{sc} and I_{scr} cells and hence the cells experienced other than particulate radiation degradation. This point will be discussed further in Section V-E.

(3) Behavior of the deviation of data points from the smooth curve in the below 8° C temperature range indicates that the extrapolated temperature correction

$$\int_{T_0}^{T} a\,dT$$

was larger than it should have been. This noted deviation was much greater for the I_{scr} cell than the I_{sc} cell.

(4) Degradation appears to be approximately 3 percent at encounter (Day 130) and 3% at the end of mission (Day 640).

2. V_{oc} Cell, Temperature Deviation. Figure 23 presents the actual and predicted output of the V_{oc} cell. The actual starts out 25 mV higher than predicted at Day 0. The deviation continually gets smaller until Day 300 where it reaches 0 mV. Following day 300 it starts increasing until it reaches a deviation of 18 mV at Day 640. In Fig. 24 V_{oc} output is converted to temperature and compared to Channel 439 actual temperature. At Day 0, V_{oc} appears to be 12° C cooler than Channel 419 temperature. The temperature difference gradually reduces to 0° at Day 300. Following Day 300 it increases and reaches 9° C at the end of mission. Excluding the first 50 days following launch, deviation between actual and predicted V_{oc} is within the anticipated accuracy of the output prediction.

E. Mariner 9, Based on Post Launch Predictions

Mariner 9 post-launch predictions are based on the temperature intensity vs time relationship displayed in Fig. 25. Predicted C 419 temperatures were used since the actual and predicted temperature profiles practically coincided. (Always within 2° C of each other.)

1. I_{sc}-I_{scr} Cells, Degradation. Figures 26 and 27 present actual and predicted outputs for the I_{sc} and I_{scr} cells, respectively. Following Day 0 normalization actual outputs were consistently lower than predicted

outputs for both cells. The ratio of predicted to actual output for both cells was computed periodically through the mission and plotted as a function of time in Fig. 28. Smooth curves were drawn through the I_{sc} and I_{scr} data. After about 200 days following launch the two curves remain approximately 3 percent apart with the I_{sc} and I_{scr} cells indicating 3 percent and 6 percent, respectively. The uncertainties in the predicted outputs associated with each curve are such that the uncertainty of each curve overlaps the other curve and thus one cannot say there is any significant difference in degradation experienced by the I_{sc} and I_{scr} cells. An average curve was plotted taking the numerical average of corresponding points on the I_{sc} and I_{scr} degradation curves. No attempt was made to weight the averages in accordance with the relative calibration uncertainties of the I_{sc} and I_{scr} cells. On March 29, 1972 an important solar array test was performed which provided a unique opportunity in the history of Mariner Spacecraft to determine in-flight the I-V characteristics of the solar array. This was done by applying various loads on the array. The predicted I-V curve was compared to the actual I-V curve and it was determined that the array had experienced approximately 3-1/2 percent current degradation since launch. This point is plotted in Fig. 28 where it is seen to be within 1 percent of the average I_{sc}-I_{scr} degradation. Several additional points are noted:

(1) All computed ratios plotted in Fig. 28 do not deviate from the average curve by more than the anticipated prediction accuracies discussed in Section IV.

(2) There appears to be no significant difference in degradation experienced by the I_{sc} and I_{scr} cells and hence the cells experienced other than particulate radiation damage. This point will be discussed further in Section V-E.

(3) Degradation appears to be approximately 4 percent at encounter (Day 168) and 4-1/2 percent at Day 480.

2. V_{oc} Cell, Temperature Deviation. Figure 29 presents the actual and predicted output of the V_{oc} cell. The actual starts out 8 mV higher than the predicted at Day 0. The deviation continually gets smaller until Day 420 where it reduces to 0 mV. In Fig. 30, V_{oc} output is converted to temperature and compared to channel 419 actual temperature. At Day 0, V_{oc}

appears to be 4° C cooler than channel 419 temperature. The temperature difference gradually reduces to 0 at Day 420. Deviation between actual and predicted V_{oc} is within the anticipated accuracy of the output prediction throughout the entire mission.

3. Mars Heating Effect. In the initial Mars orbits the array temperature was predicted to increase as the spacecraft passed near Mars sub-solar point, about 20 minutes before periapsis. Shown in Fig. 31 is how array temperatures were predicted to deviate from apoapsis temperatures as the spacecraft approached and passed through periapsis at 22-1/2 day intervals during the first 90 days in Mars orbit. Note that as the sub-solar point drifts toward periapsis, the net planet heating effect increases. Figure 32 shows the predicted planets effect at Day 320 (first day of Mars Orbit) and the actual temperatures as indicated by the temperature transducer (Channel 419), solar array (Channel 116) and the V_{oc} transducer (Channel 423). In the latter two, temperatures were deduced from voltages. The three actual temperatures tracked the predicted quite well. These same comments apply to Fig. 33 which is for Day 363 (43rd day of Mars orbit).

F. Comparison of Mariners 6, 7, and 9 I_{sc}-V_{oc} Transducers

1. I_{sc} and I_{scr} Cells, Degradation. Two important similarities are noted in the performance of the I_{sc} and I_{scr} cells on Mariners 6, 7 and 9.

(1) There appears to be no significant difference in degradation experienced by the I_{sc} and I_{scr} cells.

(2) Degradation vs time curves were similar in shape. The first similarity leads one to the conclusion that the bulk of the degradation experienced by these cells was caused by other than particulate radiation and was of a non-cell nature where "non cell" refers to the coverslide, blue-filter, anti-reflective coating and adhesives. Thus "non cell degradation" refers to output losses due to coverslide or adhesive darkening, increased surface reflection, or spectral shifts within the coverslide assembly.

The smooth average degradation (average of I_{sc} and I_{scr}) vs time curves plotted in Figs. 16, 22, and 28 are replotted in Fig. 34. Also plotted in Fig. 34 are results of an analysis on

short circuit current degradation experienced by solar arrays at synchronous attitude (Ref. 1). These two curves show the estimated "non cell degradation" experienced by the best (lowest loss) and worst (highest loss) solar arrays from a group of 15 identical satellites orbiting at near-synchronous altitudes (part of the Air Force Defense Communications Network (IDSCS)). These curves were obtained by subtracting the calculated I_{sc} degradation to cell alone due to radiation from the observed I_{sc} degradation. The Mariner curves and the IDSCS curves are quite similar as seen in Fig. 34 even though the missions were different (Mars orbiter, Mars flyby, Earth synchronous).

2. V_{oc} Cell, Temperature. The only similarity noted in the performance of the V_{oc} cell on Mariners 6, 7 and 9 was that the predicted V_{oc} cell outputs were lower than the actual outputs at earth space conditions indicating that the I_{sc}-V_{oc} transducers were cooler than temperatures indicated by the temperature transducer at earth space conditions.

VI. CONCLUSION

Based on the results presented in this report, the following conclusions are made:

(1) At earth-space conditions the I_{sc}-V_{oc} transducers are slightly lower in temperature than those indicated by the backside temperature transducers (Mariners 6, 7 and 9).

(2) There was no evidence of solar flares causing abrupt degradation (Mariners 6, 7 and 9).

(3) The transducers did not experience significant particulate radiation cell degradation (Mariners 6, 7, and 9).

(4) The transducers did experience significant "non-cell degradation" which refers to losses due to coverslides or adhesive darkening, increased surface reflection, or spectral shifts within coverslide assembly. From the available data it is not possible to determine the relative amounts of the different types of non-cell degradation. (Mariner 6, 7 and 9.)

(5) Non-cell degradation rate was highest immediately following launch. The rate steadily decreased until approximately Day 200 and then remained fairly constant thereafter (Mariner 6, 7 and 9).

(6) Mariner 6, 7 and 9 showed non-cell degradations of 3-1/2 percent, 3 percent, and 4 percent, respectively, at Mars encounter and 6 percent, 3 percent and 4-1/2 percent respectively at end of mission. (Day 720, 640 and 480, respectively.) Considering anticipated calibration uncertainty and good correlation amongst the I_{sc} and I_{scr} performance on Mariner 6, 7 and 9 spacecraft, the percent degradations mentioned above are expected to be accurate to within ±2 percent. However, it is emphasized that these anticipated accuracies were not rigorously derived, as available data (both calibration and actual) are not sufficient to establish statistically significant confidence limits describing data accuracy.

VII. RECOMMENDATIONS

Based on the analysis presented in this report the following recommendations are made regarding I_{sc}-V_{oc} transducers for future spacecraft.

(1) Select resistor values which will permit output values as high as the telemetry range will allow while considering the entire mission. Accuracy of measurement decreases below full scale.

(2) Develop a method of bonding the transducer to the base plate during calibration to effect a closer temperature control and a closer duplication of flight conditions.

(3) Incorporate a temperature transducer on the I_{sc}-V_{oc} transducer to effect better temperature data during calibration and flight.

(4) Calibrate all transducers in vacuum and bracket the entire range of predicted temperature intensity conditions for a particular mission. At each calibration intensity, vary the calibration temperature in 10°C increments from the predicted earth-space equilibrium temperature to and past the predicted equilibrium temperature corresponding to the test intensity.

(5) Repeat calibration enough times and on enough transducers to obtain sufficient data to establish statistically significant confidence limits describing the accuracy of the calibration data.

(6) Use more accurate spacecraft channels for transducer data (±1 percent).

(7) Fly a reference voltage so that telemetry accuracy can be monitored throughout the duration of a mission.

(8) Perform laboratory experiments to get a better understanding of non-cell degradation.

(9) The preceding eight recommendations have been made based on the assumption that future spacecraft will employ some type of transducer. They have been directed toward improving actual data and calibration data accuracy. However, regardless of actual data and calibration data accuracy, the transducer scheme of array performance evaluation will always have statistical inaccuracies associated with relating one cell's performance to an entire array of cells. For this reason it is strongly recommended that direct array interrogation schemes be investigated for use on future spacecraft.

REFERENCE

1. Picciano, W. T., and Reitman, R. A., Flight Data Analysis of Power Subsystem Degradation at Near Synchronous Attitude, WDL Final Report, Contract NASW-1876, Philco-Ford, Palo Alto, Calif., July 15, 1970.

Table 1. I_{sc}, I_{scr} cell temperature coefficients at 50 mW/cm^2
(average from 60°C to 0°C)

Calibration specimen	I_{sc} Cell					I_{scr} Cell				
	α	n	s	High α	Low α	α	n	s	High α	Low α
M-69 Calibration in air	0.017	10	0.004	0.027	0.006	0.046	10	0.005	0.053	0.040
S/N 001, Mariner 6	0.023	1				0.050	1			
S/N 004, Mariner 7	0.021	1				0.053	1			
M-71 Calibration in vacuum	0.028	11	0.007	0.040	0.018	0.053	11	0.006	0.062	0.044
S/N 021, Mariner 9	0.018	1				0.051	1			
Parametric data in vacuum	0.030	15								

	α	
	I_{sc}	I_{scr}
S/N 002, Calibration No. 1, air	0.039	0.062
S/N 002, Calibration No. 2, air	0.030	0.057
S/N 002, Calibration No. 3, air	0.028	0.058
S/N 015, Calibration No. 1, air	0.027	0.050
S/N 015, Calibration No. 2, air	0.023	0.058
S/N 015, Calibration No. 3, vacuum	0.038	0.061

α = Short circuit temperature coefficient in mV/°C

n = Sample size

s = Standard variance = $\dfrac{n\sum_{i=1}^{n}(\chi_i)^2 - \left(\sum_{i=1}^{n}\chi_i\right)^2}{n(n-1)}$

Table 2. Effect of variations in temperature coefficients on predicted transducer output (intensity = 50 mW/cm^2)

Transducer	Calibration No.	Output, mV		
		Reference at 60°C	Predicted at 0°C	Predicted at -30°C
I_{sc}	1 (air)	35.0	33.38	32.57
	3 (vacuum)	35.0	32.72	31.58
	% Difference	0.0	1.99	3.11
I_{scr}	1 (air)	22.0	19.0	17.5
	3 (vacuum)	22.0	18.3	16.5
	% Difference	0.0	3.52	5.88

Table 3. Deviation of prelaunch predicted from actual on "day 0"

Spacecraft	Launch date	Intensity (mW/cm^2)	Temp (°C)	Cell	Predict (mV)	Actual (mV)*	Deviation (mV)	Deviation (%)
Mariner 6	2-24-69	142.44	55	V_{oc}	527.0	532.0	-5.0	-0.9
				I_{sc}	103.3	102.4	0.9	0.9
				I_{scr}	68.1	66.7	1.4	2.1
Mariner 7	3-27-69	139.97	55	V_{oc}	518.3	545.0	-26.0	-4.9
				I_{sc}	101.4	101.2	0.2	0.2
				I_{scr}	66.8	65.7	1.1	1.67
Mariner 9	5-30-71	135.8	50	V_{oc}	520.0	528.0	-8.0	-1.5
				I_{sc}	98.2	97.5	0.7	0.7
				I_{scr}	58.8	56.5	2.3	4.1

*Actual values taken from smooth curve through incremental data points.

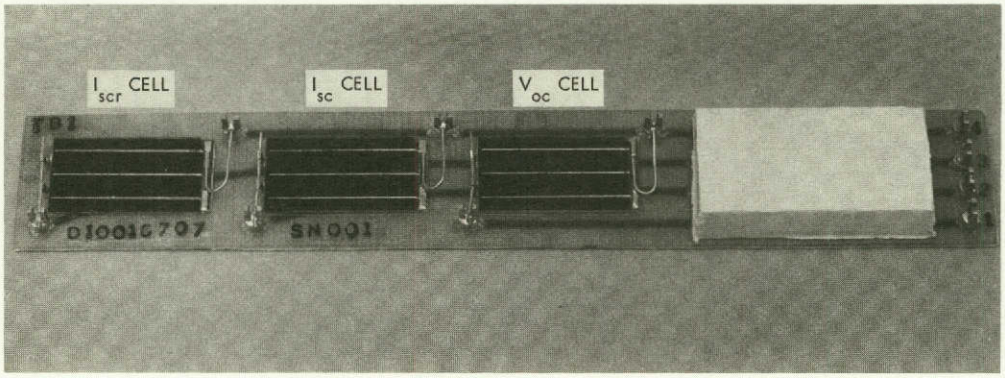

Fig. 1. Typical MM'69, MM'71 I_{sc}-V_{oc} transducer

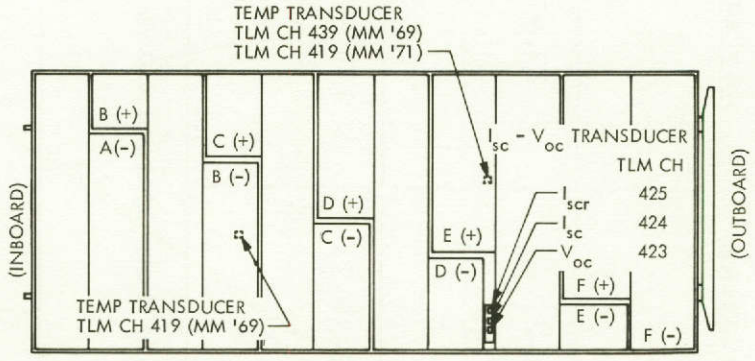

Fig. 2. MM'69, MM'71 solar panel design

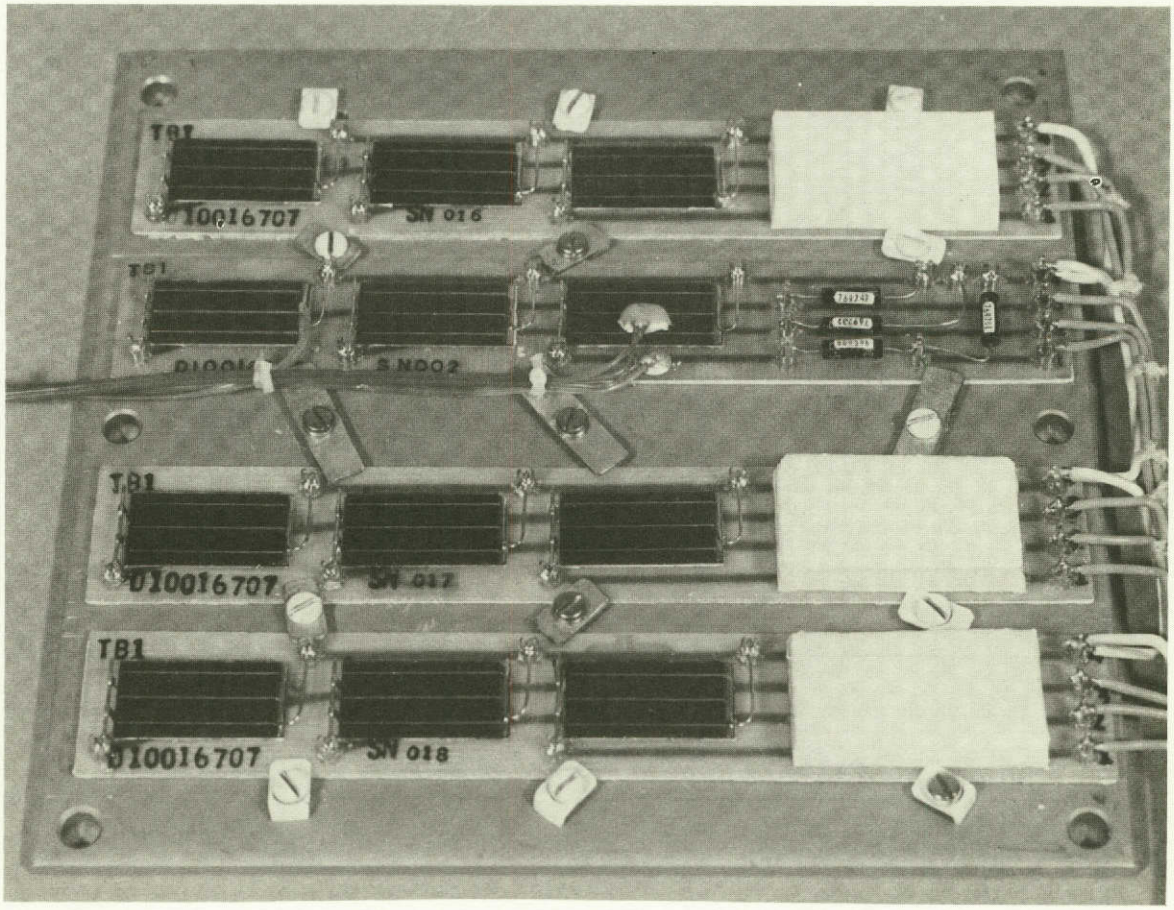

Fig. 3. Typical MM'69, MM'71 I_{sc}-V_{oc} transducer test plate

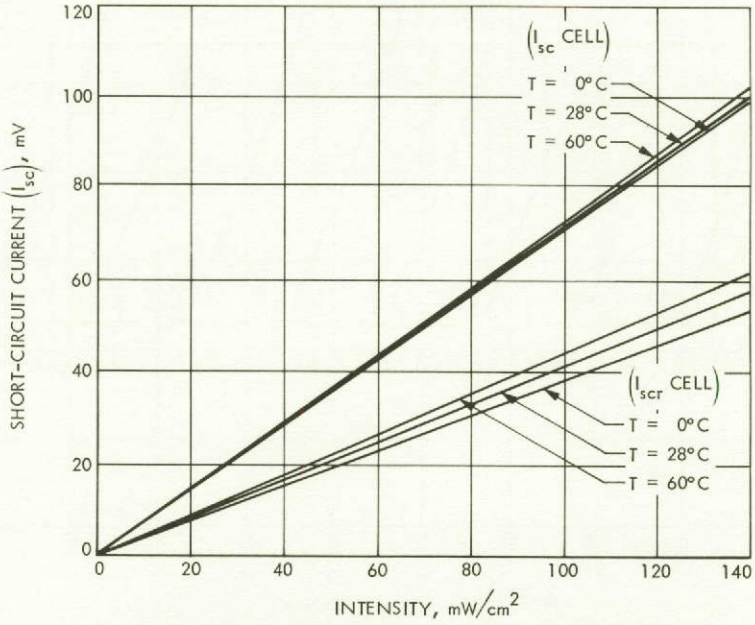

Fig. 4. Mariner 9 I_{sc}, I_{scr} pre-launch calibration

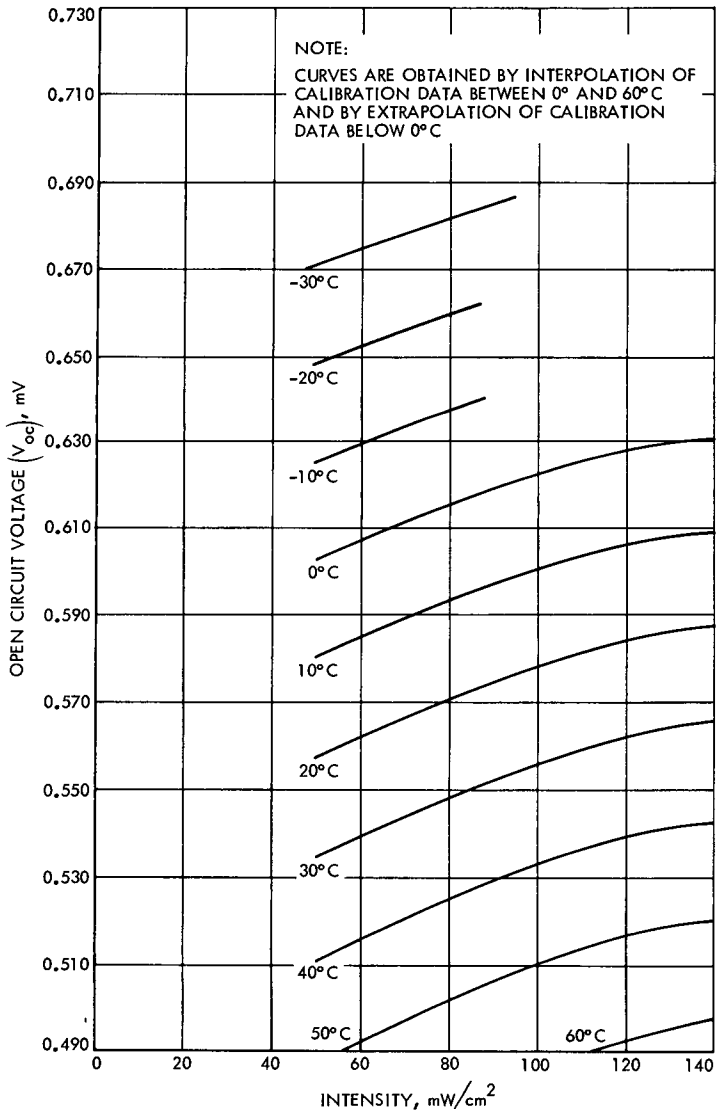

Fig. 5. Mariner 9 V_{oc} cell calibration

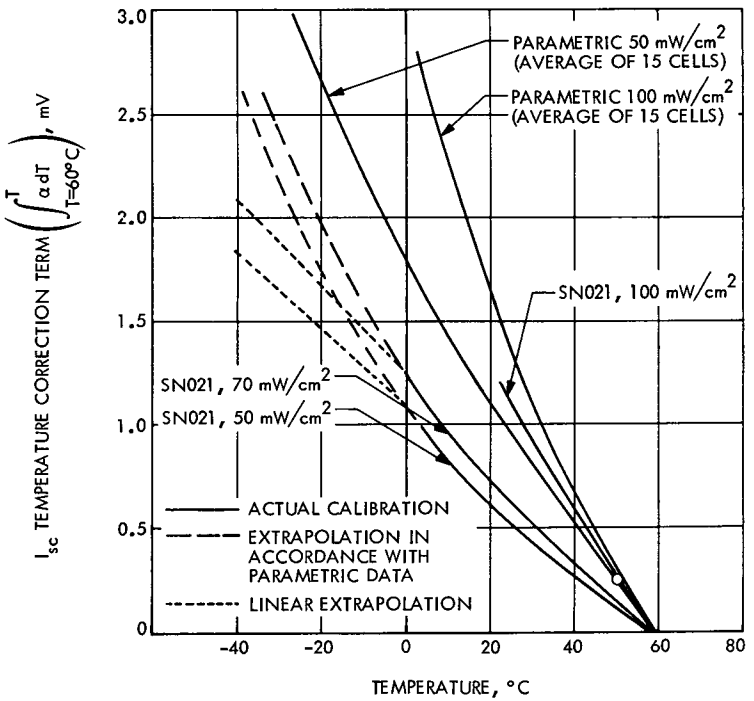

Fig. 6. Mariner 9 I_{sc} cell calibration extrapolation

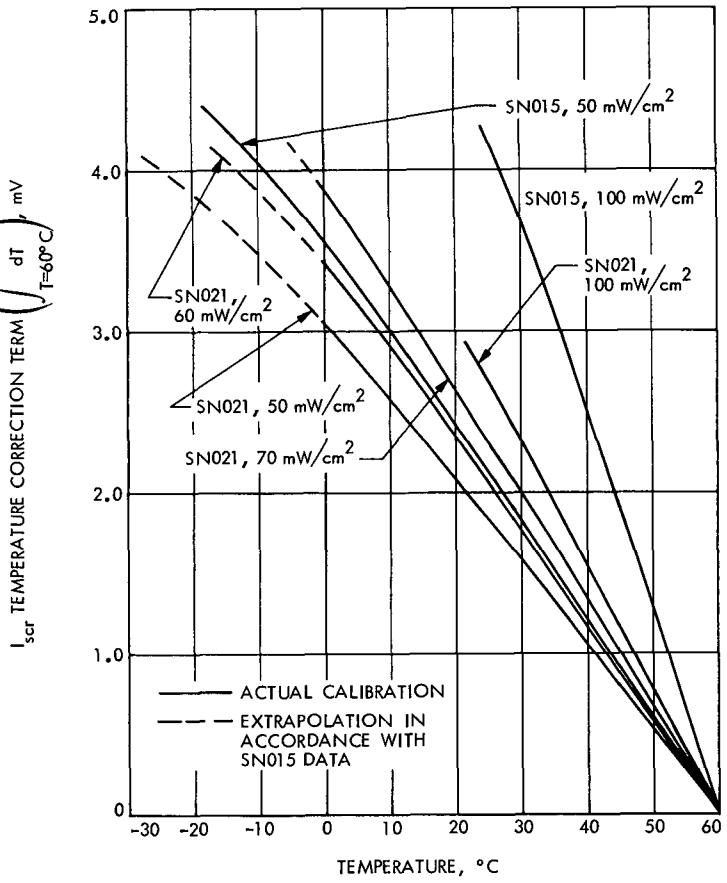

Fig. 7. Mariner 9 I_{scr} cell calibration extrapolation

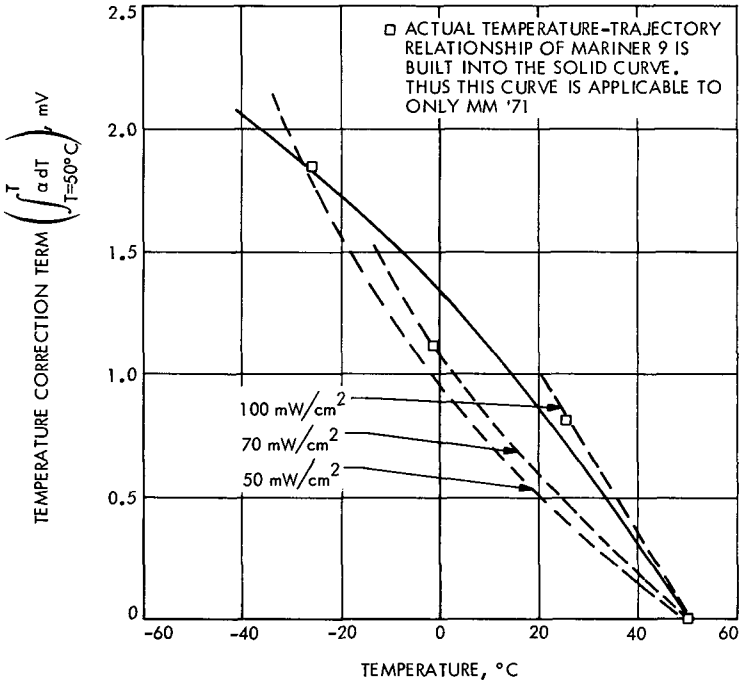

Fig. 8. Mariner 9 I_{sc} cell temperature correction term

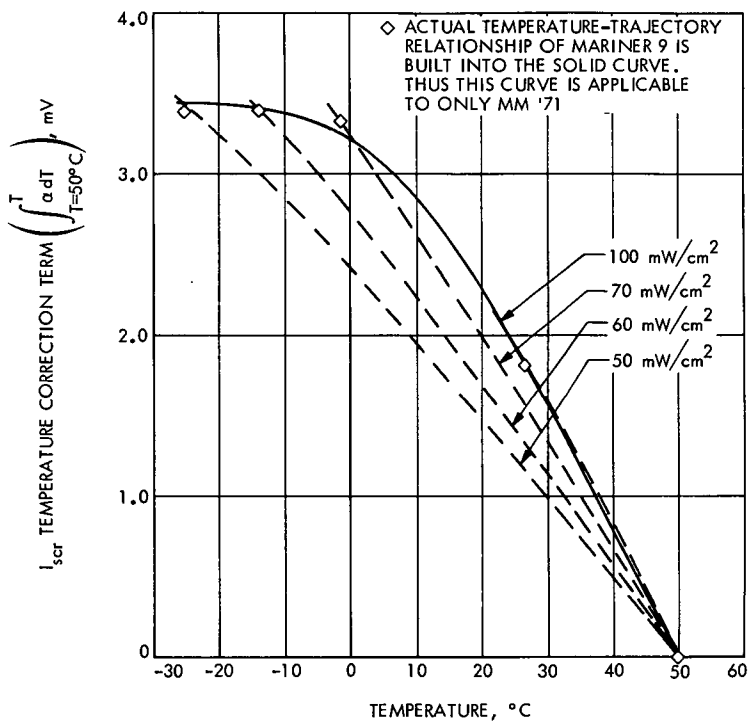

Fig. 9. Mariner 9 I_{scr} cell temperature correction term

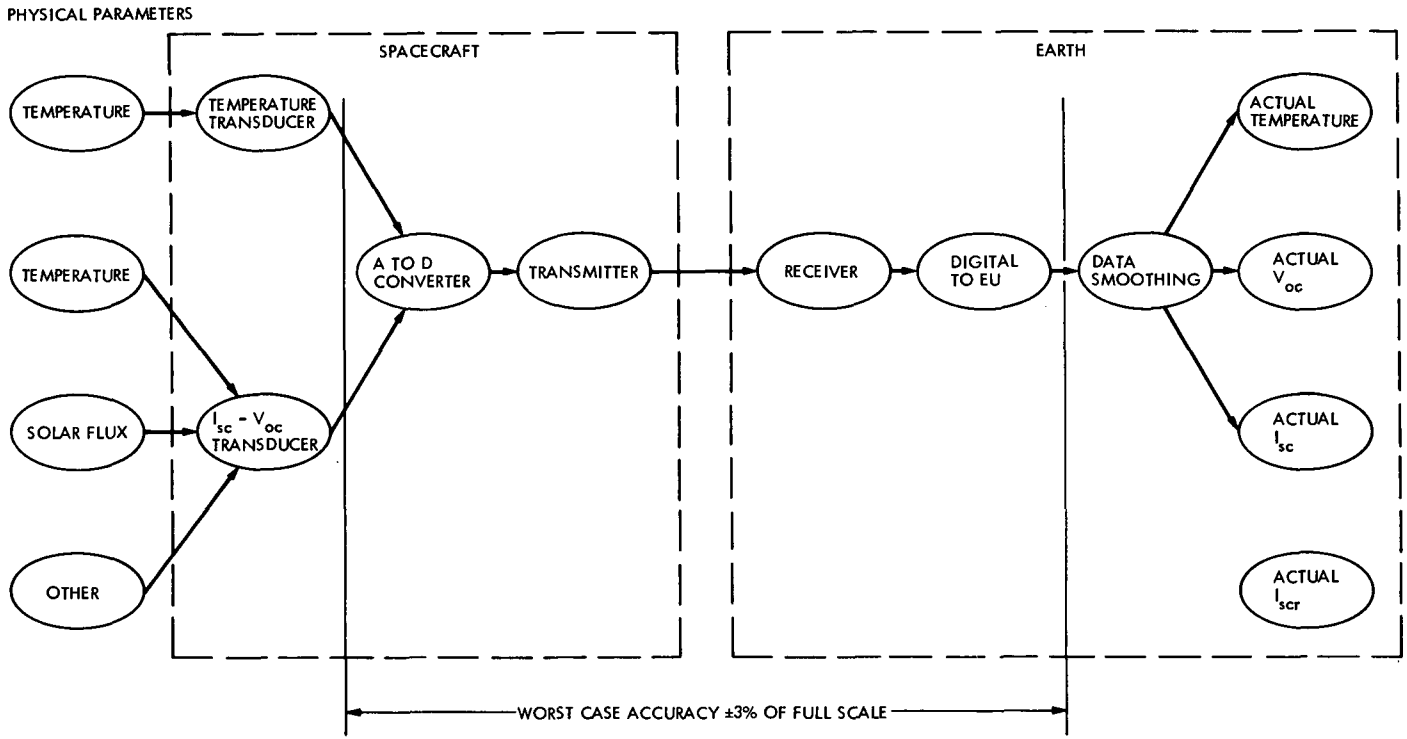

Fig. 10. Elements of I_{sc}-V_{oc} transducer and temperature transducer actual output

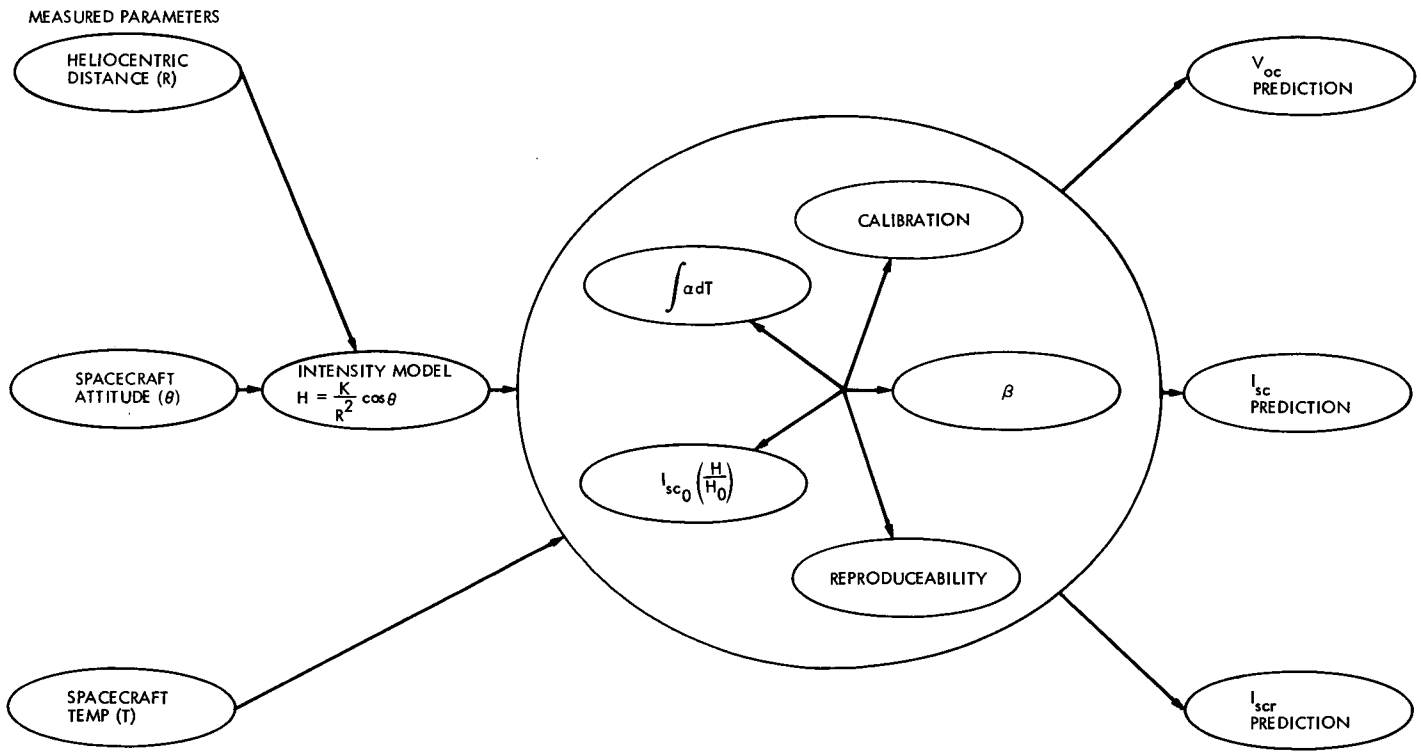

Fig. 11. Elements of I_{sc}-V_{oc} transducer predictions

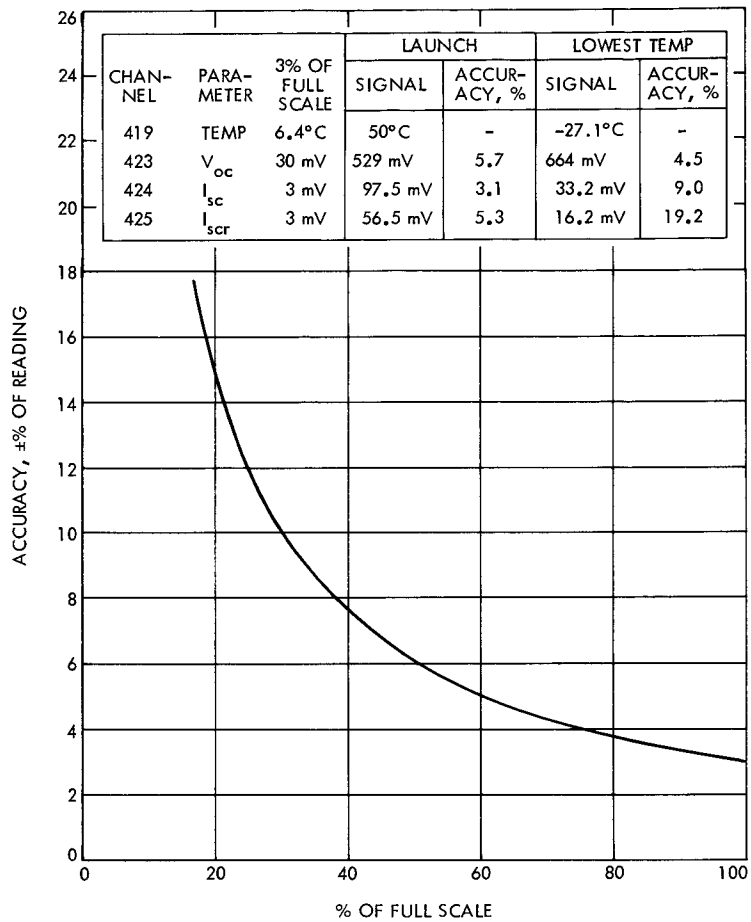

Fig. 12. Accuracy in percent for a ±3 percent of full scale channel

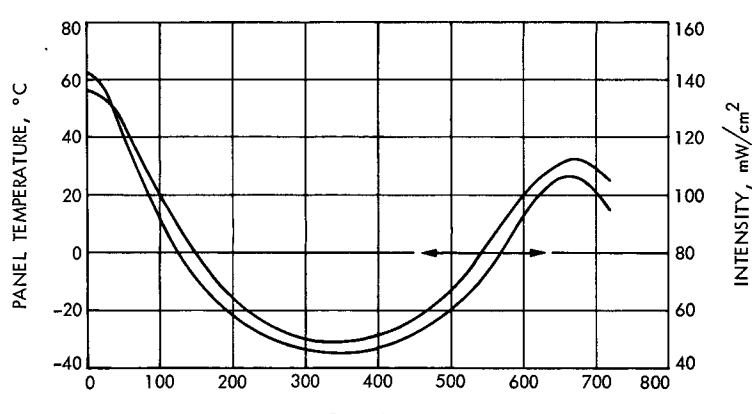

Fig. 13. Mariner 6 intensity-temperature relationship

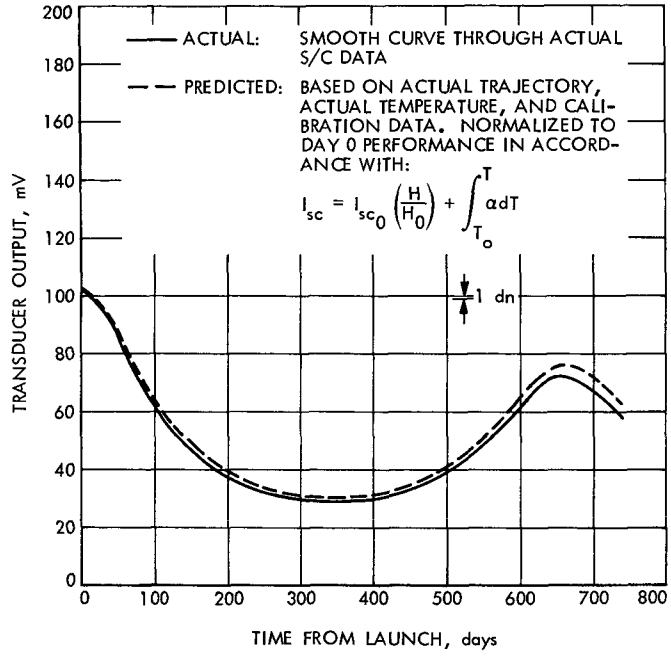

Fig. 14. Mariner 6 actual and predicted I_{sc} cell output versus time

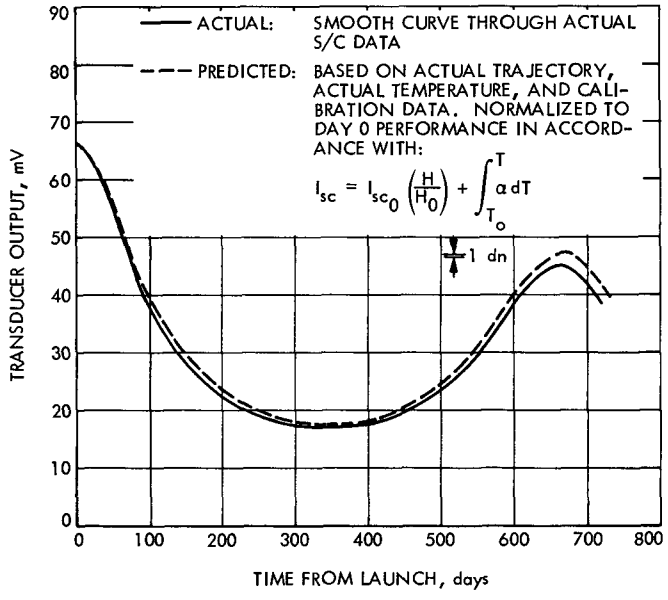

Fig. 15. Mariner 6 actual and predicted I_{scr} cell output versus time

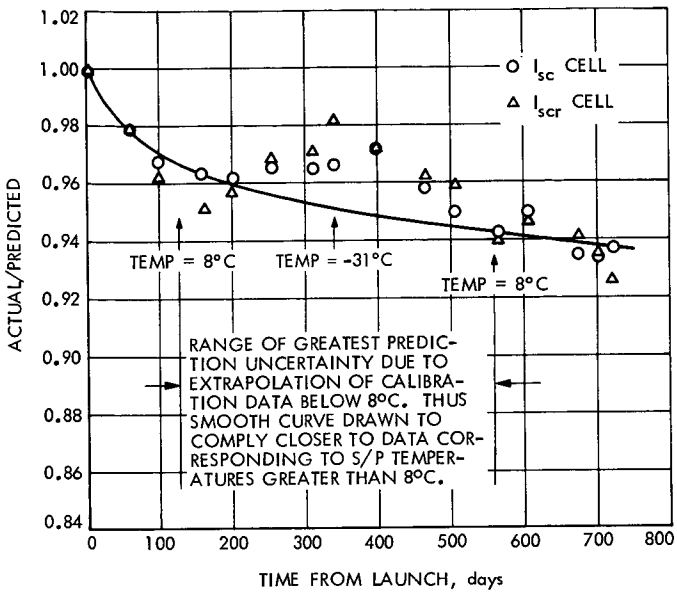

Fig. 16. Mariner I_{sc}-V_{oc} transducer current degradation

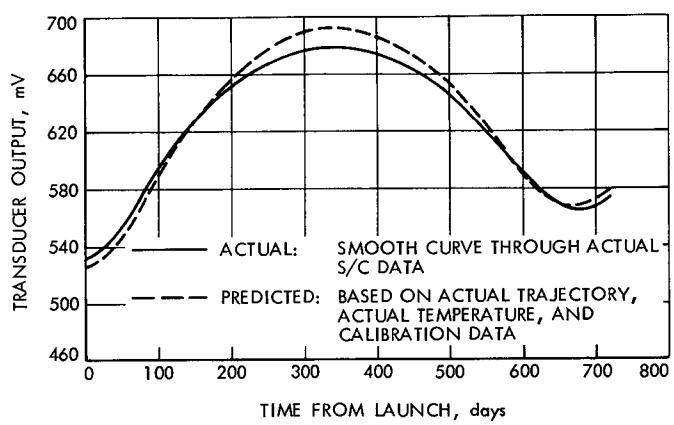

Fig. 17. Mariner 6 actual and predicted V_{oc} cell output versus time

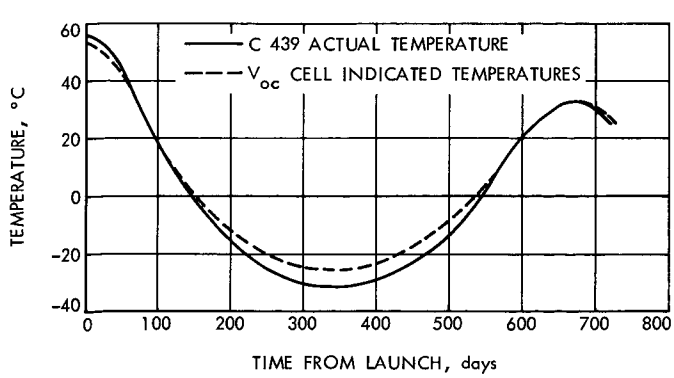

Fig. 18. Mariner 6 V_{oc} cell and C439 temperature versus time

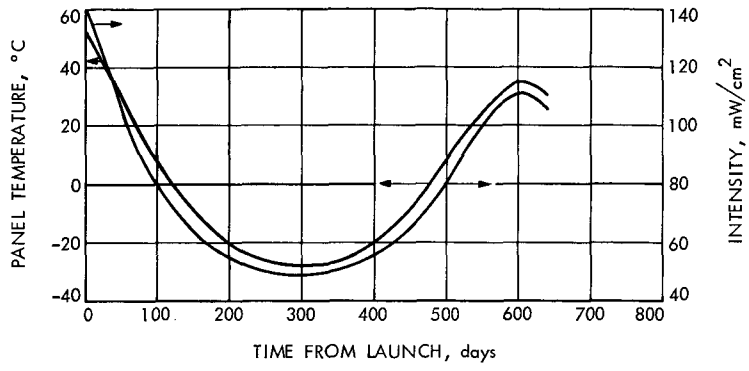

Fig. 19. Mariner 7 intensity-temperature relationship

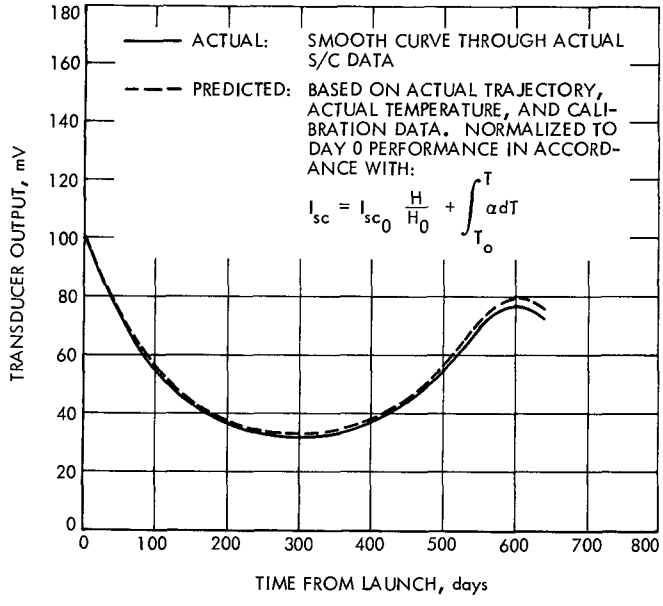

Fig. 20. Mariner 7 actual and predicted I_{sc} cell output versus time

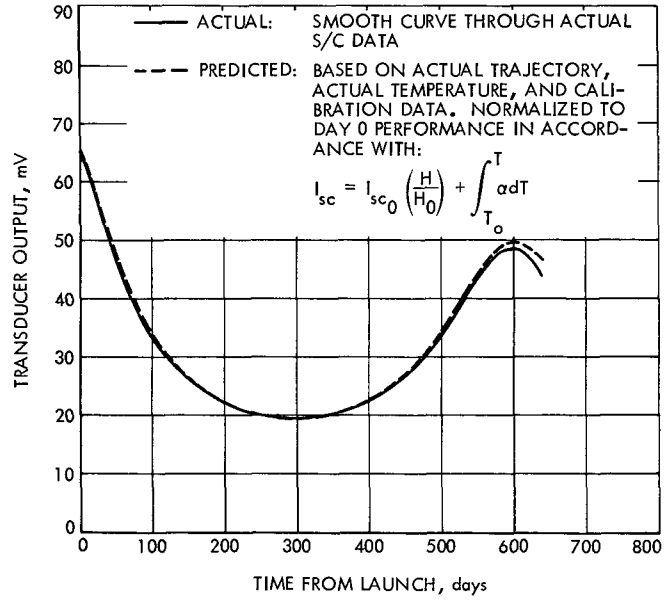

Fig. 21. Mariner 7 actual and predicted I_{scr} cell output versus time

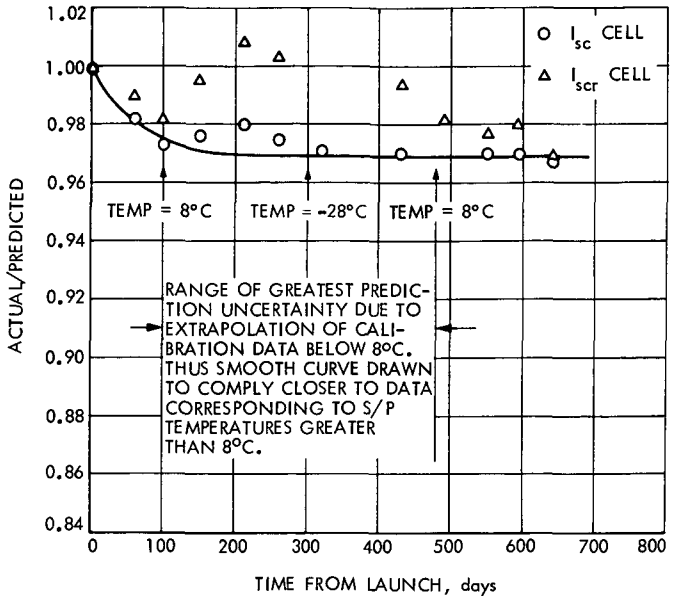

Fig. 22. Mariner 7 I_{sc}-V_{oc} transducer current degradation

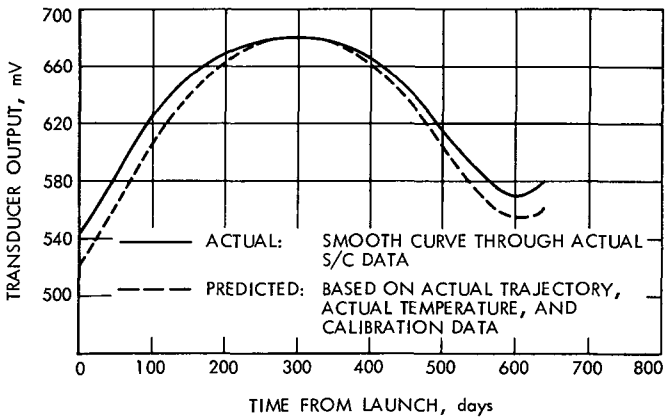

Fig. 23. Mariner 7 actual and predicted V_{oc} output versus time

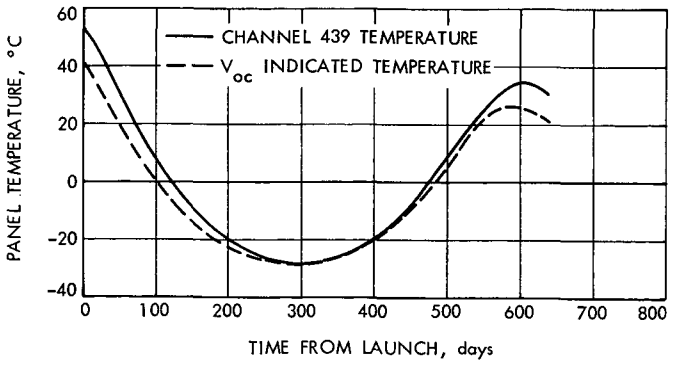

Fig. 24. Mariner 7 V_{oc} cell and C439 temperature versus time

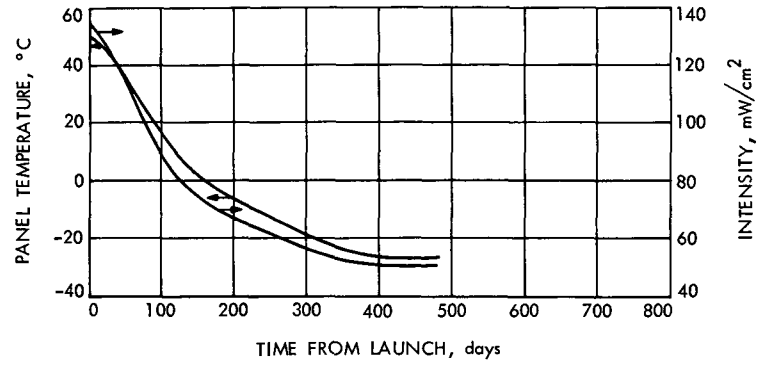

Fig. 25. Mariner 9 intensity-temperature relationship

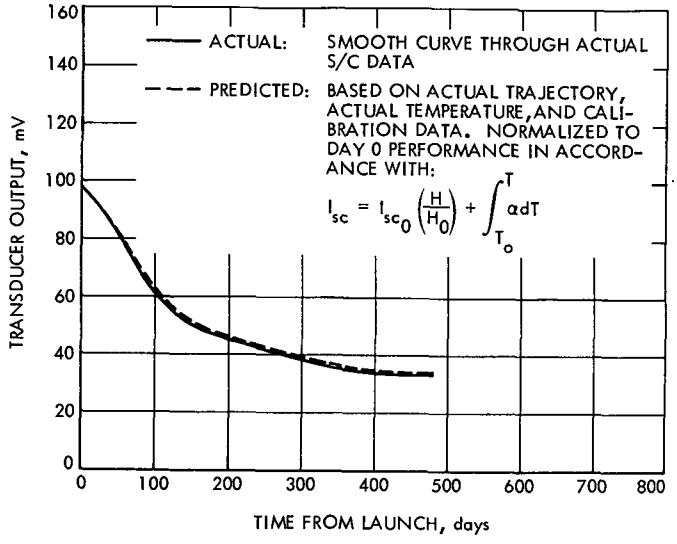

Fig. 26. Mariner 9 actual and predicted I_{sc} cell output versus time

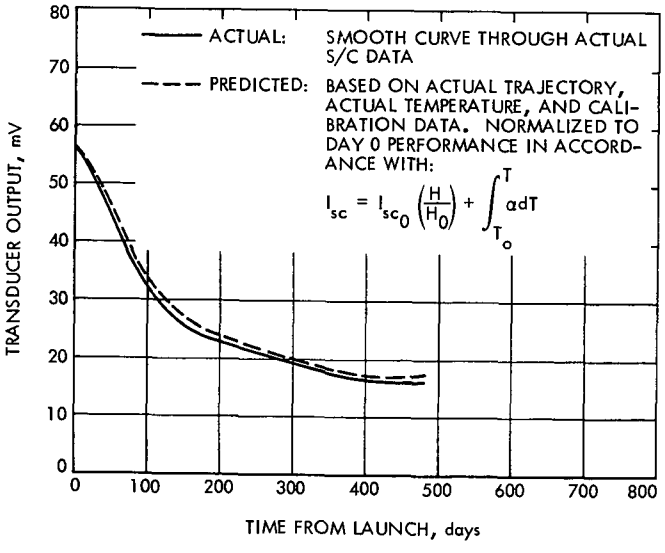

Fig. 27. Mariner 9 actual and predicted I_{scr} cell output versus time

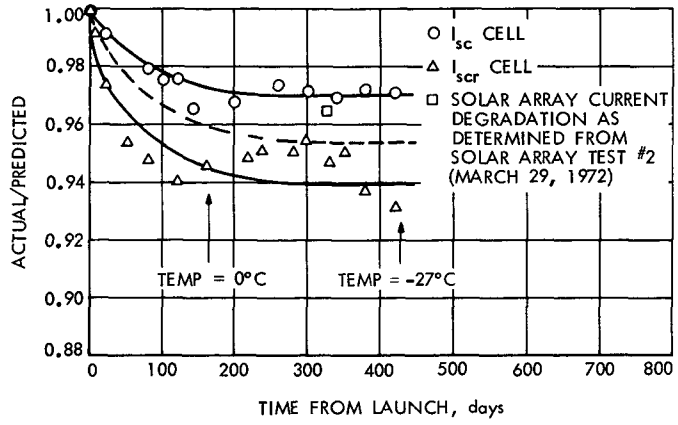

Fig. 28. Mariner 9 I_{sc}-V_{oc} transducer current degradation

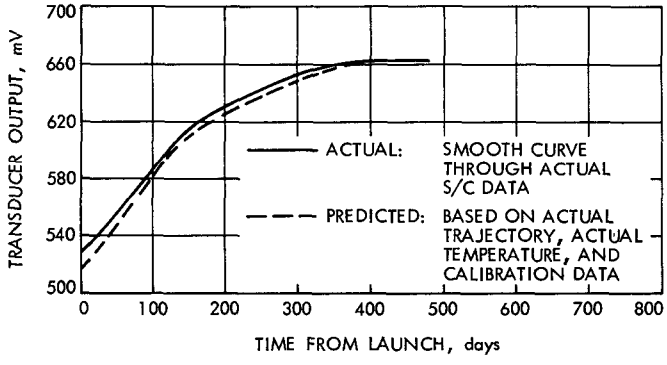

Fig. 29. Mariner 9 actual and predicted V_{oc} cell output versus time

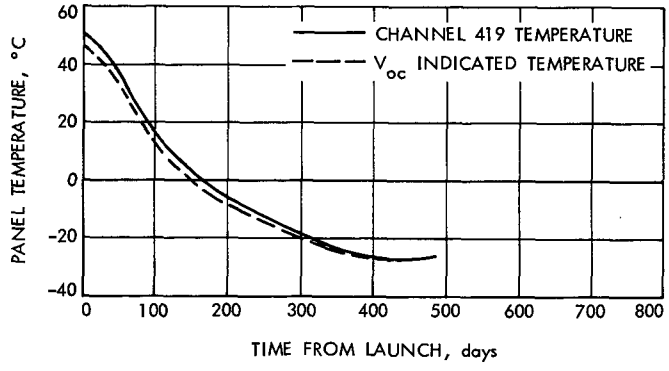

Fig. 30. Mariner 9 V_{oc} cell and C419 temperature versus time

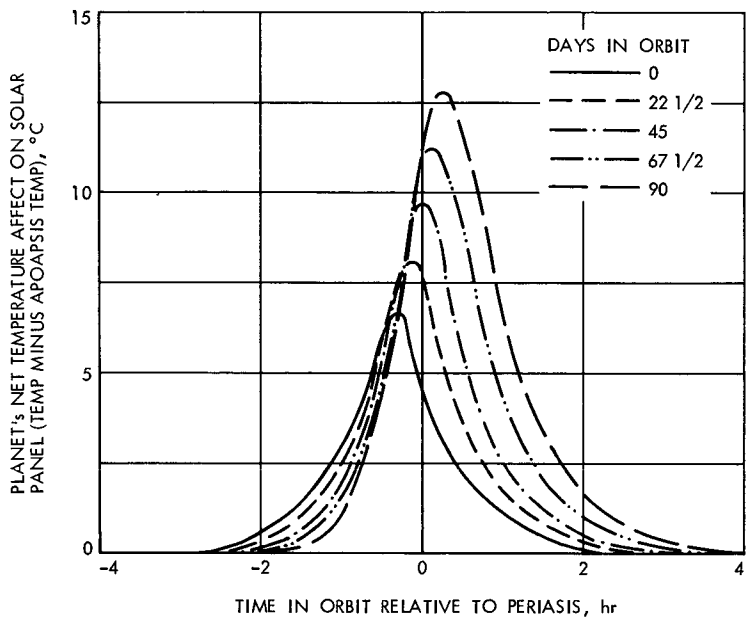

Fig. 31. Mars heating effect with days in orbit as a parameter

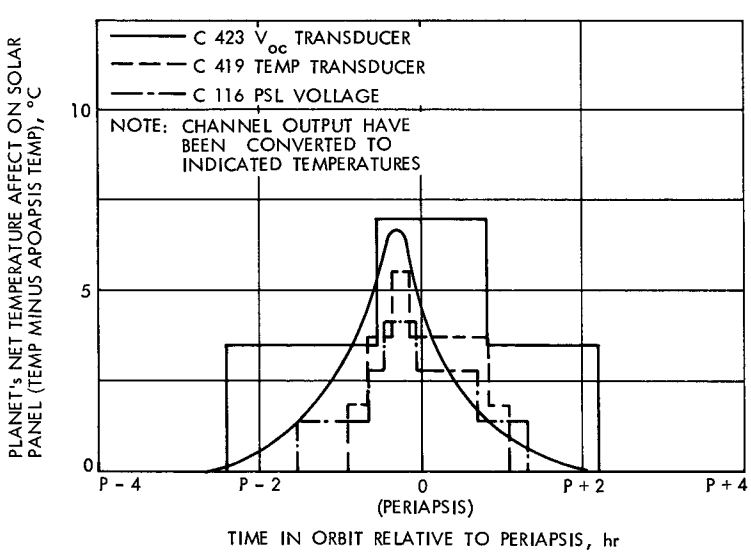

Fig. 32. Mars heating effect on channel 423, 419, and 116 during first day of orbit

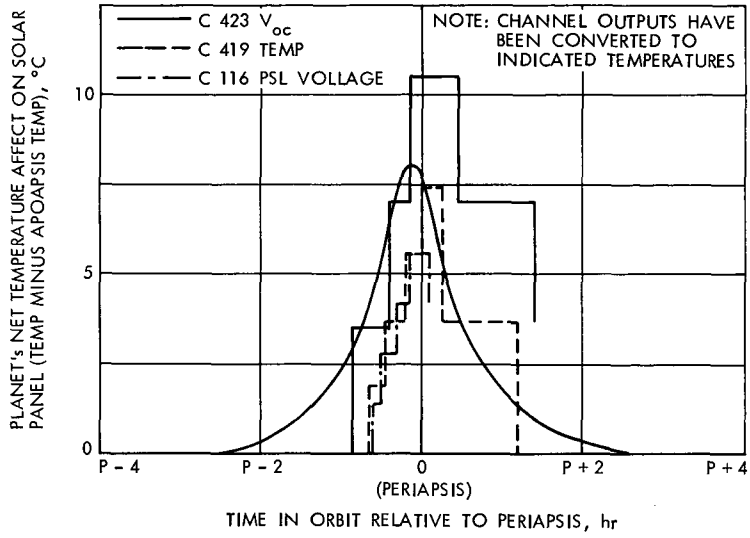

Fig. 33. Mars heating effect on channel 423, 419 and 116 during 43rd day of orbit

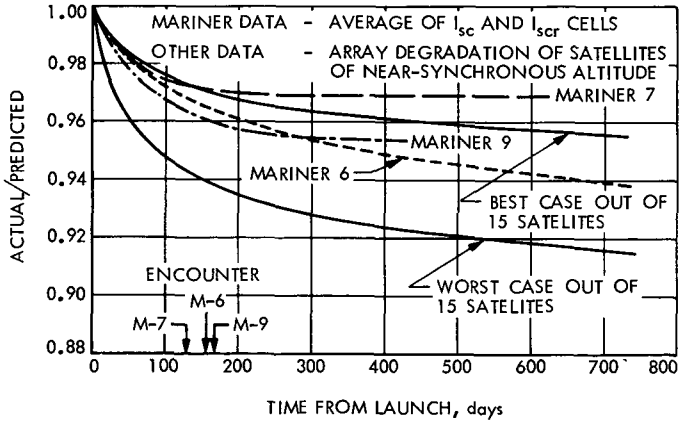

Fig. 34. Mariners 6, 7 and 9 I_{sc}-V_{oc} transducer degradation versus time

APPENDIX

Table 1A. Mariner 6 I_{sc} - V_{oc} transducer data
(S/N 001, calibrated in air)

Conditions		Calibration value, mV		
Intensity mW/cm^2	Temperature °C	I_{sc}	I_{scr}	V_{oc}
139.6	60	100.9	65.29	518.9
139.6	28	97.30	59.69	590.9
139.6	13	97.39	58.80	622.9
100.0	60	72.10	45.70	504.9
100.0	28	70.34	42.59	579.9
100.0	10	70.29	41.30	617.9
50.0	60	36.29	23.90	481.9
50.0	28	35.62	22.29	555.9
50.0	8	35.09	21.29	598.9

Table 2A. Mariner 7 I_{sc}-V_{oc} transducer data
(S/N 004, calibrated in air)

Conditions		Calibration value, mV		
Intensity mW/cm^2	Temperature °C	I_{sc}	I_{scr}	V_{oc}
139.6	60	100.00	65.00	510.9
139.6	28	96.69	59.20	581.9
139.6	13	97.39	58.00	613.9
100.0	60	72.09	45.80	498.9
100.0	28	69.99	42.25	570.9
100.0	10	69.49	40.89	608.9
50.0	60	36.09	23.89	470.9
50.0	28	35.69	22.29	546.9
50.0	8	35.00	21.10	589.9

Table 3A. Mariner 9 I_{sc} - V_{oc} transducer data
(S/N 021, calibrated in vacuum)

Conditions		Calibration value, mV		
Intensity mW/cm^2	Temperature °C	I_{sc}	I_{scr}	V_{oc}
139.6	60	101.94	61.64	497.5
139.6	28	100.10	58.07	569.9
139.6	0	99.16	54.42	630.3
100.0	60	73.03	44.00	486.4
100.0	28	71.87	41.54	560.1
100.0	0	71.05	38.44	621.8
70.0	60	50.39	30.31	473.8
70.0	28	49.82	28.43	548.7
70.0	0	49.18	26.31	611.4
60.0	60	43.49	25.78	468.3
60.0	28	42.83	24.12	543.7
60.0	0	42.16	22.28	607.1
50.0	60	36.48	21.85	462.8
50.0	28	36.12	20.45	538.8
50.0	0	35.39	18.82	602.7

NASA — JPL — Coml., L.A., Calif.